Purification and Organization of the Gene *1* Portal Protein Required for Phage P22 DNA Packaging†

Christopher Bazinet,‡ Julyet Benbasat,§ and Jonathan King*

Department of Biology, Massachusetts Institute of Technology, Cambridge, Massachusetts 02139

José Maria Carazo and José L. Carrascosa

Centro Biologia Molecular, Universidad Autonoma de Madrid, Madrid, Spain

Received July 13, 1987; Revised Manuscript Received November 3, 1987

ABSTRACT: The gene *1* protein of *Salmonella* bacteriophage P22 is located at the DNA packaging vertex of the mature particle. The protein is incorporated into the procapsid shell during shell assembly and is required for DNA packaging. The unassembled precursor form of the gene *1* protein has been purified from cells infected with mutants blocked in procapsid assembly. The purified 90 000-dalton protein was dimeric or monomeric; upon storage in the cold it formed 20S cyclic dodecamers. Computer filtering of negatively stained electron micrographs revealed 12 arms and knobs projecting from a central ring, with a 30-Å channel at the center. Similar dodecameric rings were released from disrupted procapsid shells. These results indicate that the gene *1* protein is organized as a cyclic dodecamer within the procapsid shell and serves as the portal through which P22 DNA is threaded during DNA packaging. The presence of a 12-fold ring located at a 5-fold portal vertex appears to be a conserved structural theme of the DNA packaging apparatus of double-stranded DNA phages.

Though the overall symmetry of the capsids of dsDNA phage is described as icosahedral, all of the dsDNA phages have a unique vertex which is differentiated from the remaining 11 vertices. This vertex, termed the portal or DNA packaging vertex, is recognizable in the mature virus as the site of tail attachment (Murialdo & Becker, 1978a; Tsui & Hendrix, 1980; Black & Showe, 1983; Bazinet & King, 1985). During assembly this vertex serves as the site for the packaging of newly replicated DNA into the precursor shell. Later in the life cycle it is the channel through which the DNA exits from the capsid shell and passes into the infected cell (Black & Showe, 1983; Bazinet & King, 1985).

This vertex is marked by a unique protein species not found at the other vertices, the portal protein. During DNA packaging soluble packaging proteins bind to the *pac* site (or in the case of λ, the *cos* site) on the newly replicated DNA (Earnshaw & Casjens, 1980; Feiss & Becker, 1983). This protein/DNA complex docks at the DNA packaging vertex of the precursor shell and in an ATP-dependent reaction pumps the DNA into the shell (Hsiao & Black, 1977; Feiss & Becker, 1983; Georgopoulos et al., 1983). The portal protein is thought to participate in these docking functions (Hsaio & Black, 1978b; Murialdo & Becker, 1978a,b; Earnshaw & Casjens, 1980; Black & Showe, 1983; Bazinet & King, 1985a).

The portal vertex is the site of the symmetry mismatch between the 6-fold rotational symmetry of the tails of dsDNA phages and the 5-fold rotational symmetry of icosahedral vertices (Moody, 1965). Hendrix (1978) proposed that the mechanism of DNA packaging involves rotation of the portal ring with respect to the shell. In this model the symmetry mismatch provides the conditions allowing subunits to slide past each other.

Studies of a number of different bacteriophages indicate that procapsid assembly is initiated at the portal vertex [T4: Laemmli and Eiserling (1968), Muller-Salamin et al. (1977), Yanagida et al. (1984), and Hsiao and Black (1978a). λ: Murialdo and Becker (1977, 1978b) and Kochan et al. (1984). φ29: Hagen et al. (1976) and Camacho et al. (1977)]. We have been particularly interested in the mechanism by which the portal protein is assembled into only one of 12 presumably equivalent vertices. If the portal protein subunits are not tightly bonded to the capsid, the specificity of its location at a single vertex becomes even more problematic.

In bacteriophage T4 the portal protein is the product of gene *20* (Muller-Salamin et al., 1977; Hsaio & Black, 1977; Driedonks et al., 1981); in bacteriophage λ it is the gene *B* and *B** proteins (Tsui & Hendrix, 1980; Kochan et al., 1983). In bacteriophage φ29 it is the gene *10* protein (Carrascosa et al., 1982, 1983). In bacteriophage P22 this protein is the product of gene *1* of the phage (King et al., 1973; Hartwieg et al., 1986). The λ gene *B* protein, the T4 gene *20* protein, the φ29 gene *10* protein, and the T3 gene *8* protein (Carazo et al., 1986a) all are found as disk-shaped oligomers with 12 knobs or arm-like structures projecting radially outward from a central ring, through which a channel of 3–5 nm in diameter is visible in electron micrographs.

The T4 portal protein is required for procapsid initiation and is itself organized on the host cell membrane (Hsiao & Black, 1978a; Driedonks et al., 1981; Black & Showe, 1983). The λ portal protein is apparently organized in concert with the host groE protein and is also covalently modified during morphogenesis (Kochan & Murialdo, 1983; Kochan et al., 1984). In contrast, the P22 portal protein does not appear to be required for procapsid assembly and is not covalently processed during morphogenesis (King et al., 1973; Bazinet & King, 1987). This raised the question of its macromolecular

† Supported by National Institutes of Health Grant GM 17980 to J.K. and by the Comision Asesora de Investigaciôn Cientifica y Tecnica, Spain (J.L.C.).

* Author to whom correspondence should be addressed.

‡ Present address: Department of Developmental Genetics and Anatomy, Case Western Reserve University, Cleveland, OH 44106.

§ Present address: Department of Microbiology, University of British Columbia, Vancouver, British Columbia, Canada.

0006-2960/88/0427-1849$01.50/0

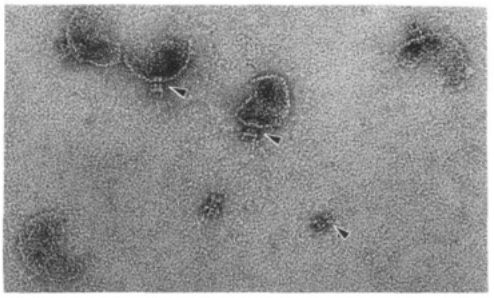

FIGURE 1: DNA injection apparatus of mature P22 particles. Mature phage have been disrupted by heating. The arrow points to the disc-shaped structure composed of the gene *1* protein (Hartwieg et al., 1986). The precursor form of this protein, prior to its assembly into virus particles, is the material whose purification is reported herein.

organization within the procapsid.

Bacteriophage P22 is an icosahedral phage whose genetics, protein composition, and intracellular assembly have been defined in considerable detail (Botstein et al., 1973; Susskind & Botstein, 1978; King et al., 1976; Fuller & King, 1982). The precursor to the mature particle is the double-shell procapsid, which is empty of DNA (King et al., 1973; Casjens & King, 1974). The major components of the procapsid are 420 copies of the gene *5* coat protein, 250 copies of the gene *8* scaffolding protein, and 10 ± 3 copies of the gene *1* polypeptide chain (King & Casjens, 1974; Fuller & King, 1981). However, no morphologically distinct portal vertex has been observed in electron micrographs of procapsids (Lenk et al., 1975; Fuller & King, 1981).

As a result of their stability and isometric morphology, both the mature shells and the precursor shells have been studied by low-angle X-ray scattering (Earnshaw et al., 1976; Earnshaw & King, 1978) and also by Raman spectroscopy (Thomas et al., 1982). Of particular advantage for biochemical studies is the absence of proteolytic or other covalent modifications during assembly of the proteins into the virus particle; all the transformations are at the level of conformation and subunit–subunit interaction.

The 90000-dalton gene *1* protein is a minor component of both the procapsid and the mature phage, present in 10 ± 3 copies/shell (King et al., 1973; Casjens & King, 1974). In disrupted mature P22 capsids (Figure 1), it is found as a disk-shaped structure lying within the shell at the tail-attachment vertex (Hartwieg et al., 1986). If the gene *1* protein is removed by mutation, closed procapsid shells of coat and scaffolding protein form, but these are not competent in DNA packaging since they lack the portal for DNA entry (Botstein et al., 1973; Poteete et al., 1979).

In this paper we report the purification of the precursor form of the gene *1* protein of P22 and its spontaneous assembly in vitro into disk-shaped oligomers with the same dimensions as those observed in partially disrupted phage structures.

Experimental Procedures

Bacterial and Phage Strains. All strains are from the collections of D. Botstein or J. King. Host strains are derived from *Salmonella typhimurium* LT2. The su$^-$ host DB7000 and its *Sup*E derivative DB7004 have been described previously (Susskind et al., 1974). Phage were derivatives of P22 *c1-7*. The amber mutations utilized are described in Botstein et al. (1973) and Poteete and King (1977). The gene *1* mutation *dif1* was found as a secondary mutation carried by a gene *14* amber mutant *14$^-$amH638* (Youderian & Susskind, 1980; Bazinet & King, 1985b). Particular strains are specified in the detailed descriptions of the experiments in which they were used.

Purification of the Gene 1 Portal Protein. Bacteria (DB7000) were grown to a concentration of 3 × 10^8 cells/mL in super broth (Fuller & King, 1981) and infected at a multiplicity of infection (moi) of 10 phage/cell with P22 *5$^-$amN114/13$^-$amH101/c1-7* or P22 *1$^-$amN101/5$^-$amN114/13$^-$amH101/c1-7* and incubated at 25 °C for 3 h with vigorous aeration. Cultures were then cooled to 4 °C on ice (with aeration).

All subsequent steps were carried out at 0–4 °C. After being pelleted by low-speed centrifugation (10 min, 4000 rpm in the Sorvall GSA rotor), cells were concentrated 100-fold in ice-cold buffer M [50 mM tris(hydroxymethyl)aminomethane hydrochloride (Tris-HCl), pH 8.0, 2 mM disodium ethylenediaminetetraacetate (Na_2EDTA), 3 mM 2-mercaptoethanol, 0.2 mM phenylmethanesulfonyl fluoride (PMSF), 0.1% NaN_3, 1% (v/v) glycerol], frozen in a liquid nitrogen bath, and then stored at −20 °C. The highly viscous lysate obtained after gentle thawing was passed twice through a French pressure cell at 15000 psi. Large debris were pelleted by centrifugation in the Sorvall SS34 rotor (20 min at 15000 rpm). The supernatant was then centrifuged in a Beckmann type 50 rotor for 2.5 h at 40000 rpm.

After dialysis against three changes of buffer B10 [50 mM Tris-HCl, pH 7.4, 2 mM EDTA, 3 mM 2-mercaptoethanol, 0.1% NaN_3, 10% (v/v) glycerol] for a minimum of 3 h each, the high-speed supernatant was applied to a DEAE-cellulose column (DE-52, Whatman) equilibrated in the same buffer. The column was eluted with a 50–300 mM NaCl gradient. The gene *1* protein was observed to elute from the DE-52 column at relatively high salt concentrations, between 160 and 220 mM NaCl. Fractions containing the gene *1* protein [as judged by sodium dodecyl sulfate–polyacrylamide gel electrophoresis (SDS–PAGE) of fractions from *1*$^-$- and *1*$^+$-infected cells prepared in parallel] were pooled.

Ammonium sulfate (13.7 g) was added to the gene *1* protein (gp*1*) pool (95 mL), and the mixture was left overnight at 4 °C. The precipitate was pelleted by centrifugation for 100 min (Sorvall SS34 rotor, 8000 rpm) and resuspended in buffer B10. This material was then applied to a Bio-Gel A0.5m (1.5-cm i.d., 40 cm long) column in the same buffer. Fractions containing gp*1* were pooled and reprecipitated by the addition of ammonium sulfate to 37.5% saturation. After being pelleted by centrifugation as described above, gp*1* was redissolved in buffer B10. Protein was stored at 4 °C. Protein was determined by the method of Bradford (1976).

Rate–Zonal Sedimentation of gp1. Gene *1* protein (120 μg) was dialyzed against buffer B1 [same as buffer B10, except that the glycerol was adjusted to 1% (v/v)] overnight at room temperature. As a sedimentation standard, 120 μg of purified gp*9*, the tailspike protein of phage P22 (Berget & Poteete, 1980), was added to each sample. Samples were applied to the tops of linear 5–20% sucrose gradients prepared in the same buffer and centrifuged at 34000 rpm for 15 h at 4 °C in the Beckman SW50.1 rotor. Twenty fractions of equal volume were collected from each gradient through a hole in the bottom of the tube, and the locations of the proteins were determined by SDS–polyacrylamide gel electrophoresis (Laemmli, 1970). After being stained with Coomassie blue (Fairbanks et al., 1971), proteins were quantitated on a Joyce-Loebl scanning microdensitometer.

Analytical Gel Exclusion Chromatography of gp1. Approximately 150 μg of gp*1* was combined with a mixture of proteins used as gel filtration size standards (Bio-Rad Laboratories) and P22 phage. A total sample of 280 μL was applied to the top of a Bio-Gel A0.5m column (40 cm × 1.5-cm i.d.)

and eluted with buffer B10 at constant pressure. Protein was detected by absorbance at 280 nm and by SDS–polyacrylamide gel electrophoresis of column fractions.

Partial Dissociation of 2⁻ Procapsids for Electron Microscopy. Procapsids were purified from cells infected with P22 *2⁻amH200/13⁻amH101/c1-7* as described by Fuller and King (1982). After treatment with 0.5 M guanidine hydrochloride (Gdn-HCl), which releases the bulk of the scaffolding protein from the procapsids, shells were separated from soluble scaffolding protein by differential centrifugation in the Beckman Type 50 rotor for 45 min at 40 000 rpm, 4 °C. The bulk of the gp*1* remained associated with the shells (Fuller & King, 1981). The supernatant, which contained some gp*1*, was dialyzed against 20 mM KPO_4, 1% (v/v) glycerol, and 2 mM EDTA, pH 7.4 (three buffer changes, 4 °C), and fractionated through a phosphocellulose column (Whatman, P11) equilibrated with the same buffer. Scaffolding protein is bound to the column. Residual shells, slightly enriched in gp*1* (2–5-fold), were recovered in the column eluate.

Electron Microscopy. Samples were applied to carbon-coated 400-mesh copper grids freshly exposed to glow discharge. Grids were stained with 2% uranyl acetate, and structures were visualized on a JEOL 100B transmission electron microscope, with an accelerating voltage of 80 kV. In some cases the material to be examined was first applied to a surface of freshly cleaved mica and stained by the method of Horne and Ronchetti (1974). For the measurements of the portal rings, magnification was calibrated by inclusion of bacteriophage T4 particles, by use of the 4.1-nm spacing of the annuli of the tail sheath (Moody, 1973).

Image Processing. Good images showing front views of the portal rings were digitized in a Perkin-Elmer 1010A flat-bed microdensitometer with a square window of 25 μm on a side (corresponding to 0.55 nm on a specimen) and a sampling interval equal to the window size. The picture's gray-level scale was linear in the optical density of the micrographs.

Individual Rotational Analysis. Eleven isolated specimens, all of them contained in the same micrograph, were visually selected for image processing on the basis of rotational analysis techniques. This approach first requires the selection of the specimen's point that is going to be considered as the center for the Fourier series expansion of the image in the angular polar coordinates (Crowther & Amos, 1971). This center was approximately located on the specimen with the help of an interactive display system and was further refined by a multiple-step procedure. First a center was found that minimized the power of the order 1 harmonic component all over the specimen. This latter center and the one obtained visually were compared to the ones resulting from the minimization of the order 1 harmonic component over the inner specimen region (between 8 and 21 pixels over a total diameter of 43 pixels) and over the outer one (between 25 and 40 pixels), separately. Only pictures in which these four centers were within less than 2% of the total specimen diameter were further considered. Three pictures were disregarded at this step. The finally considered center for the Fourier series expansion was the one that minimized the eccentricity all over the specimen. The Fourier expansion was thus independent of the symmetry of the specimen.

Following this procedure, the center that maximized the 12-fold symmetry of the specimen in the outer region was calculated. In all but one case (that was not considered further in this work), this center was very close (within less than 2% of the total specimen diameter) to the one obtained by minimization of the eccentricity of the specimen. The same also happened when the center that maximized the 6-fold symmetry of the specimen in the inner region was considered in all cases in which a significant 6-fold component was found (in all but three cases). These results indicated that the minimization of the eccentricity of the specimen implied a maximization of the 12-fold as well as the 6-fold symmetry.

The rotational filtering was carried out by allowing only selected rotational components to have nonzero coefficients at all radii in the Fourier series expansion of the picture.

Average Image. Once the Fourier series expansion of each one of the seven pictures previously referred to was calculated, they were averaged to obtain a single final image. The relative phase difference of each harmonic component with respect to a fixed spatial direction (the origin of the angular coordinate) was calculated; this indicates the relative axial orientation of different harmonics in the same or in different images. In the latter case much care was taken to ensure that the reference spatial direction was the same for all images [For a more detailed study of this kind, see Carazo et al. (1984)].

The basis for this averaging was the existence of a clear 12-fold symmetry in all the specimens studied and also the existence of a significant 6-fold symmetry in most of the individual specimens. In practice, the averaging process was as follows: The picture showing the most relevant 6-fold and 12-fold rotational components was chosen as the reference picture (picture "a"). The correlation over the outer specimen region of the 12-fold rotational component between the reference picture a and another different picture of the selected set (picture "b") was calculated. Picture b was rotated the angle α needed to get a correlation maximum of the 12-fold component, obtaining a rotated picture designated by b_1; picture b was also rotated by the angle α of +90°, obtaining picture b_2. Pictures (a, b_1) and (a, b_2) were then averaged, and the power spectra of the final pictures were calculated. Both averaged pictures showed a clear and enhanced 12-fold component, but in one case the 6-fold rotational component was almost eliminated while in the other one it was notably enhanced. The latter image, showing enhanced 12-fold and 6-fold rotational symmetries, was considered more representative of the true structure of the specimen on the basis of the rotational power spectra (Crowther & Amos, 1971) of the individual specimens and was further processed as the reference picture. This procedure was repeated with each one of the selected pictures, yielding the finally averaged image. A control of the possible systematic errors introduced by the choice of the first reference picture was carried out by repeating the whole process, considering two other images as first reference pictures. The results obtained were essentially the same, indicating the consistency of the procedure.

RESULTS

Purification of the Gene 1 Protein of Bacteriophage P22. In order to purify the gene *1* protein, cells were infected with P22 phage carrying multiple mutations intended to maximize the yield of gp*1* in precursor form. The clear plaque mutation in the *c1* gene ensures entry into the lytic cycle, so that late proteins will be synthesized in all infected cells. The *5⁻* nonsense mutation prevents synthesis of the major capsid protein, resulting in the accumulation of the other virion proteins in unassembled form. The *13⁻* nonsense mutation delays cell lysis, allowing synthesis of phage proteins to continue for several hours beyond the normal lysis time.

Major steps in the purification of the protein were high-speed differential centrifugation, DEAE-cellulose ion-exchange chromatography, ammonium sulfate precipitation, and gel exclusion chromatography. A protein with the same mobility

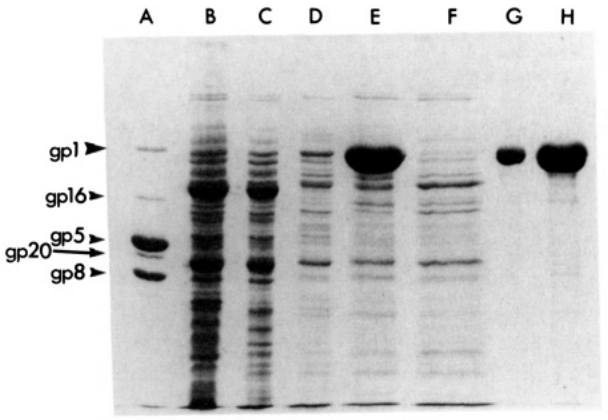

FIGURE 2: Purification of the gene *1* protein monitored by SDS–polyacrylamide gel electrophoresis. Samples from successive stages during the purification of the gene *1* protein were assayed for electrophoretic homogeneity. The gel shown here was stained with Coomassie blue. (A) Purified 2^- procapsids; (B) low-speed supernatant; (C) high-speed supernatant; (D) pool from DE-52 ion-exchange chromatography; (E) ammonium sulfate precipitate; (F) ammonium sulfate precipitate from a $1^-/5^-$ lysate prepared in parallel; (G) pool after Bio-Gel A0.5m gel filtration chromatography, 8 μg of protein loaded; (H) same as (G), 40 μg loaded.

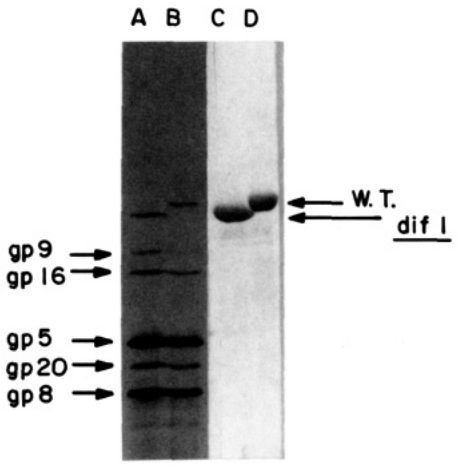

FIGURE 3: Purification of a mutant gene *1* protein. The left-hand lanes are autoradiograms of procapsids isolated from infected cells incubated with ^{14}C-labeled amino acids. (A) Procapsids containing the *dif1* protein; (B) procapsids containing wild-type gp*1*. The right-hand lanes show the proteins purified from cells infected with strains blocked in capsid assembly following the protocol described under Experimental Procedures and in the text. (C) Purified *dif1* protein; (D) purified wild-type gene *1* protein. The procapsids from the *dif1* mutant infected cells have the gene *9* tailspikes associated with them. Normally, the tailspikes add to mature capsids in the last step phage assembly. We observed premature association of tailspikes with *dif1*-containing structures in a number of preparations.

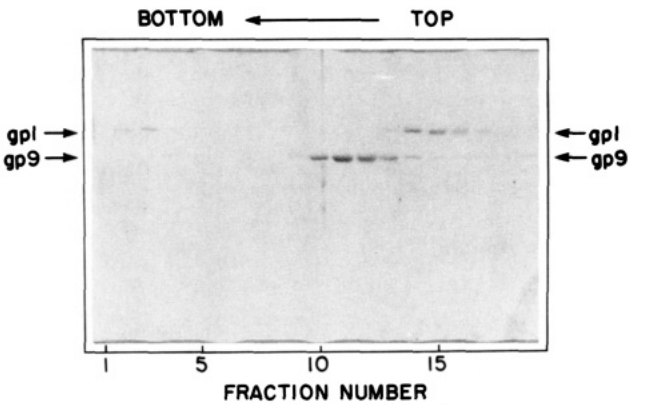

FIGURE 4: Rate–zonal centrifugation of purified gene *1* protein. Sedimentation is from the right to the left in the figure. The portal protein sedimented in two discrete peaks, centered around fractions 2 and 15. Purified gp*9* (Berget & Poteete, 1980) was added as a sedimentation standard.

in SDS–polyacrylamide gel electrophoresis as gp*1*, absent from lysates of 1^--infected cells, was purified as described under Experimental Procedures. Figure 2 shows the results of SDS gel electrophoresis of material at several different stages of the purification process. We estimate that the final product is greater than 90% pure. From 3 L of infected cells, approximately 6 mg of gp*1* was recovered. A control 1^- amber preparation was brought through the purification process in parallel. Lane F shows that the 92 000-dalton protein purified from the $1^+/5^-$-infected cells was missing from this 1^- preparation, consistent with its identification as the product of gene *1*.

The final step of the purification was gel filtration chromatography through a precalibrated Bio-Gel A0.5m (exclusion limit ~500 000 daltons). The protein was recovered from the included volume of this column. This suggested that the protein had been recovered in an unassembled form, probably as a monomer or dimer.

To confirm that this species was the gene *1* product, we took advantage of a gene *1* mutation, *dif1*, which alters the electrophoretic mobility of the protein in SDS gels. This mutant protein is functional and assembles into infectious particles. Cells infected with P22 $dif1/5^-/13^-$ were subjected to the purification protocol described above. As shown in Figure 3, the purified protein that emerged had the mobility of *dif1*; there was no band with the mobility of the wild-type protein. This established that the protein we have purified is the product of gene *1*.

Oligomerization of the Gene 1 Protein in Vitro. The sedimentation of gp*1* through sucrose gradients was studied with the rate–zonal method of Martin and Ames (1961). The protein used in this experiment was pooled from fractions included in a Bio-Gel A0.5m column (exclusion limit approximately 500 000 daltons). One species of gp*1* sedimented more slowly than gp*9*, in a peak with a sedimentation coefficient of approximately 5S–7S (Figure 4). For a 90 000-dalton protein, this is consistent with a monomeric or dimeric state, depending on the frictional coefficient. Another species sedimented as a discrete peak near the bottom of the centrifuge tube. This protein sedimented about twice as far as the control tailspikes on the same gradient. Since tailspikes have a sedimentation coefficient of 9.3S (Berget & Poteete, 1980), we estimate that the fast sedimenting species of gp*1* has a sedimentation coefficient of approximately 20S.

The protein analyzed by sedimentation had been stored for 2 weeks at 4 °C. After storage for another 5 weeks, a sample of the preparation was applied to the same Bio-Gel A0.5m column that had included all of the gp*1* during the purification procedure. The bulk of the gp*1* was excluded by the gel filtration column (Figure 5), indicating that the protein had aggregated into structures larger than the 0.5 million dalton exclusion limit of the column.

Electron Microscopy of the Gene 1 Protein. When the stored protein was examined under the electron microscope, regular ring-shaped structures of uniform size and morphology were observed (Figure 6). These structures have the morphology of a stain-excluding inner ring, with a stain-penetrated channel through its center. Extending radially outward from the inner ring are a number of arm-like projections, with a thickening at the end which gives the appearance of a second, outer ring of protein. Occasional images appeared to be portal rings lying on edge, with the central channel extending across the particle image.

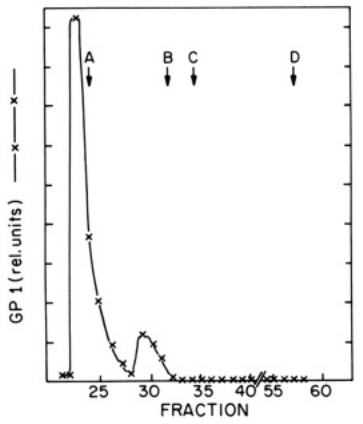

FIGURE 5: Gel filtration chromatography of portal protein. (×) Relative optical density of gp*1* bands after SDS gel electrophoresis of column fractions. The arrows at fractions 24, 32, 35, and 57 represent elution peaks of (A) thyroglobulin, M_r 670 000 (Edelhoch, 1960), (B) bovine γ-globulin, M_r 158 000 (Hess & Deutsch, 1948), (C) ovalbumin, M_r 44 000 (Edsall, 1953), and (D) vitamin B_{12}, M_r 1350 (Hodgkin et al., 1955).

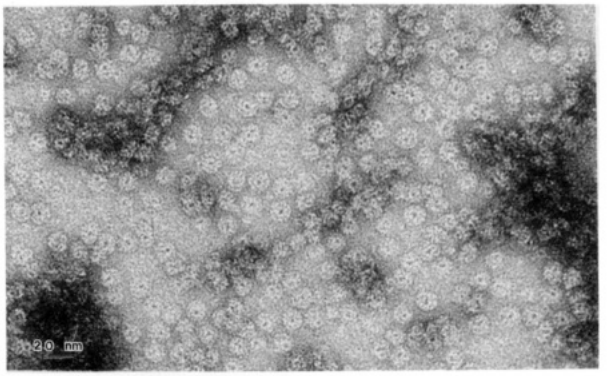

FIGURE 6: Electron micrograph of purified portal structures. The structures have been negatively stained with uranyl acetate. Radial arms projecting out from a central annulus can be discerned on many of the particles. Occasional particles appear to be lying on their sides, with a stain-penetrated channel crossing the structures.

The dimensions of the structures observed are summarized in Figure 11. They are similar to those reported for the gp*1* disk observed at the top of the tail structure recovered from mature phage disrupted by being heated in the presence of EDTA (Hartwieg et al., 1986). The best views of the portal structure in negative stain strongly suggest that the structure has 12-fold rotational symmetry, like the portal proteins of phages T4 (Driedonks et al., 1981), φ29 (Carazo et al., 1985), λ (Kochan et al., 1984), and T3 (Carazo et al., 1986a).

Portal Structure in Capsids Assembled in Vivo. The structure assembled in vitro by the gene *1* protein was a good candidate for the disc structure observed at the portal vertex of mature phage (Hartwieg et al., 1986). However, a differentiated vertex with a portal structure has not been observed in electron micrographs of procapsids.

Treatment of procapsids with 0.5 M guanidine hydrochloride causes the release of the scaffolding protein but leaves the portal protein associated with the coat protein shell (Fuller & King, 1981). We therefore examined a sample of procapsid shells that had been partially disrupted by guanidine treatment and separated from the released scaffolding protein by phosphocellulose chromatography. The resulting electron micrographs reveal the presence within procapsids of a structure very similar in morphology to those which we have observed in the purified portal preparations. Treatment of the proheads with guanidine also caused the release of intact portal structures from some of the capsids (Figure 7). Thus, the

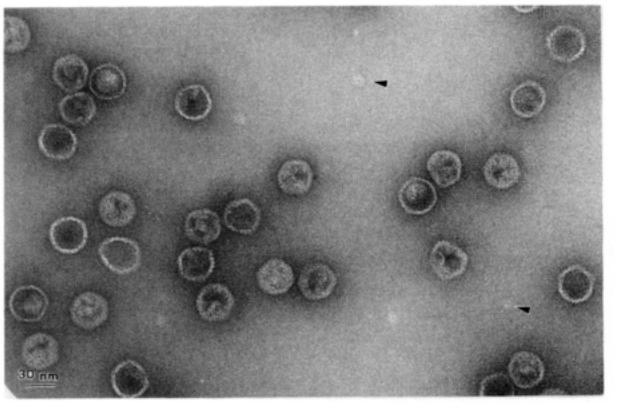

FIGURE 7: Visualization of portal structures from partly dissociated procapsids. The supernatant from high-speed differential centrifugation of guanidine-treated procapsids was fractionated through a phosphocellulose column, which binds scaffolding protein (gp*8*) but not residual capsids and portal structures. Portal structures can be seen lying free on the surface of the grid (arrows). Occasionally, the portal structure could be visualized directly within the guanidine-treated capsid lattice (as in the procapsid in the lower left corner of this figure).

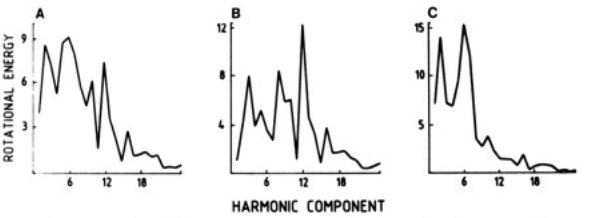

FIGURE 8: Rotational power spectrum from a single portal image. These figures display the strengths of the intensities found as a function of the repeat around the cyclic images (Crowther & Amos, 1971). (A) Power spectrum of the whole particle structure; (B) power spectrum calculated from the outer specimen region (between radii of 25–40 pixels); (C) power spectrum from the inner region (8–21 pixels).

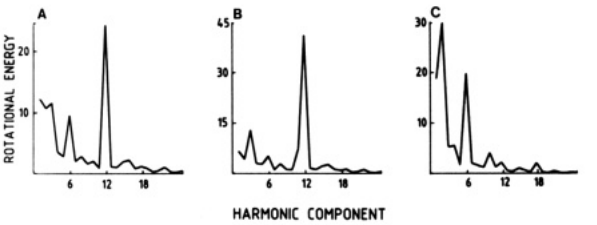

FIGURE 9: Rotational power spectra of the averaged image. (A) Power spectrum corresponding to the entire structure; (B) outer region; (C) inner region.

portal structures assembled in vitro closely resemble those recovered from biologically active procapsids assembled in vivo.

Rotational Analysis and Filtering. Negatively stained images of the rings formed from purified portal protein were selected for computer filtering as described under Experimental Procedures. The rotational analysis of the individual portals showed a rotational power spectrum with an important 12-fold symmetry (Figure 8A), especially in the outer region (Figure 8B), and a significant 6-fold component in the inner region (Figure 8C) in most of them. These features were enhanced in the rotational spectrum of the final averaged image. Figure 9A shows the total power spectrum of the rotationally averaged image, while Figure 9B shows the outer specimen region and Figure 9C shows the inner region.

These symmetries were clearly visualized in the average rotationally filtered image (Figure 10). This latter image shows 12 knobs of density in the outer region, 6 density maxima in the inner region, and a hole in the center. Each knob presumably corresponds to a domain of a single gp*1*

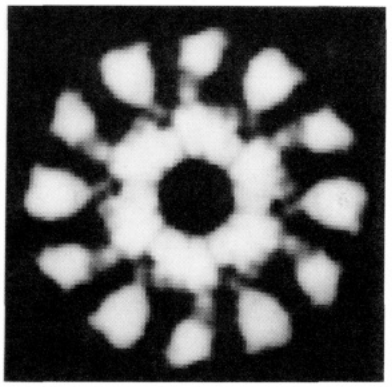

FIGURE 10: Rotationally filtered portal structure. This image was derived by averaging selected images and then rotationally filtering the average image as described under Experimental Procedures.

molecule. The 6-fold symmetry of the inner ring suggests that the annulus-forming domain of the molecule is dimer clustered. The 30-Å channel is wide enough to allow passage of a double-stranded DNA molecule (Earnshaw & Casjens, 1980).

Other features in this image include the modulation of the six density maxima in the inner region and the appearance of two somewhat different types of density maxima in the outer region, which are produced by the presence of a small 12-fold harmonic component in the inner region and another, also small, 6-fold harmonic component in the outer region. However, on the basis of the power spectra shown in Figure 8 these are probably not significant features of the structure.

Discussion

The purified gene *1* portal protein was isolated from infected cells in which capsid assembly was blocked by a nonsense mutation in the gene coding for the major coat protein. As initially purified, the protein was probably a monomer or dimer. After concentration and storage in a low-salt buffer at 4 °C, the subunits spontaneously assembled into cyclic oligomers. These structures had 12 spokes and knobs projecting from a central annulus (Figures 10 and 11). Each knob and spoke projecting from the central ring presumably represent one domain of a 90 000-dalton gp*1* chain. The remaining portion of the molecule is intimately associated with neighboring portal protein domains in the central ring.

Though not evident morphologically in the intact procapsid shell, the release of dodecameric complexes from disrupted procapsids (Figure 7) indicates that the portal protein is organized in that form within the procapsid. Assuming that each of the 12 morphological units of the portal disk represents one portal polypeptide chain, the structure accounts for all of the 10 ± 3 gene *1* polypeptides in each procapsid and mature phage particle (Casjens & King, 1974). Thus a unique portal vertex is already defined in the otherwise icosahedral procapsid (Earnshaw et al., 1976).

The morphology of this structure immediately suggests a role for the gp*1* ring as the specific channel through which the DNA is translocated during the DNA encapsidation process. Recent experiments indicate a direct role for gp*1* in DNA packaging; a missense mutation in gene *1* results in the production of P22 particles with a higher density of packaged DNA (S. Casjens, M. Hayden, and E. Wyckoff, personal communication).

The knob and spoke domains probably interact with the coat and scaffolding subunits in the procapsid shell. During DNA packaging the complex of the gene *2* and *3* proteins with the *pac* site on the concatemeric DNA presumably docks at the stem of the portal structure (Poteete et al., 1979; Casjens &

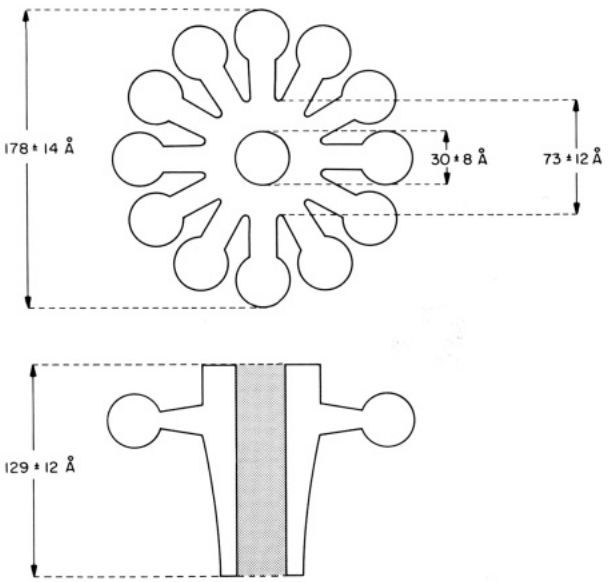

FIGURE 11: Diagram of the gp*1* portal structure. (Top) Face-on view, down the axis of rotational symmetry; (bottom) side view. Dimensions for the inner channel, inner ring, and outer radius are based on an average of 56 measurements, ±SD. Length of channel is based on 19 measurements.

Huang, 1982; Casjens et al., 1987). In the mature shell, which lacks the scaffolding subunits, these domains would be interacting with the coat subunits alone. After DNA packaging the products of genes *4*, *10*, and *26* close the DNA packaging channel and form the neck of the phage (Strauss & King, 1984). These proteins probably bind around the stem of the portal structure.

The oligomeric form of the protein was quite stable once formed. On passage through a gel filtration column the rings remained intact. The cyclic structures also survived the Gdn-HCl treatment used to disrupt procapsids. Since the protein as purified from infected cells was not oligomerized, it was presumably unassembled within the infected cells. The normal assembly pathway probably requires interaction of the portal subunits either with coat and scaffolding subunits or with the growing procapsid shell, rather than the incorporation of a preformed dodecameric ring (Bazinet & King, 1987).

The two most effective purification steps were DEAE-cellulose ion-exchange chromatography and ammonium sulfate precipitation. Relatively high concentrations of salt were required to elute portal protein off the DE-52 column, indicating the presence of an acidic domain. However, the protein was precipitated at a lower ammonium sulfate concentration than the other proteins in the pooled DE-52 fractions, consistent with the presence of a hydrophobic region. Separate charged and hydrophobic domains in the free subunits might correspond to the outer knob and inner annulus domains in the assembled form.

The structures are similar in size and distinctive morphology to the disk-like structures observed at the top of the DNA injection apparatus derived from mature phage particles (Hartwieg et al., 1986). During the DNA packaging process the capsid shell expands about 10% (King et al., 1974). The measurements of the mature ring are not precise enough to determine whether the portal dimensions remain constant during these transformations or whether the portal ring also changes.

The portal structures of T4 (Driedonks et al., 1981), $\phi 29$ (Carrascosa et al., 1985), λ (Kochan et al., 1984), and T3 (Carazo et al., 1986a) also have 12-fold rotational symmetry. A three-dimensional reconstruction from electron micrographs

has been carried out for phage ϕ29 portal protein at 1.8-nm resolution (Carazo et al., 1986b). The reconstruction shows clearly the collar-like projections of the inner radius. The similarity in morphology of the portal structures from the four phages, despite considerable variety in the mechanisms by which they are assembled, supports the idea that the DNA packaging mechanism is the same in the various dsDNA phages (Earnshaw & Casjens, 1980). The protein cleavage associated with the portal protein of λ appears to be a secondary process, since the ϕ29, T4, and P22 proteins have similar morphologies and functions.

The symmetry mismatch between the 12-fold portal structure and the 5-fold capsid vertex is also a conserved feature of double-stranded DNA phage structure. This suggests some general functional significance, perhaps the necessity for the portal structure to rotate with respect to the vertex during the DNA packaging or injection processes, as suggested in the model of Hendrix (1978).

ACKNOWLEDGMENTS

Part of this work was done in a collaborative research project between the CBM and the IBM Madrid Scientific Centre. We thank Erika Hartwieg for expert assistance with electron microscopy and Peter Prevelige for scaffolding-depleted procapsid shells. We are grateful to Sherwood Casjens, Melody Hayden, and Elizabeth Wyckoff for communication of unpublished data.

REFERENCES

Adams, M. B., Brown, H. R., & Casjens, S. (1985) *J. Virol. 53*, 180–184.

Bazinet, C., & King, J. (1985a) *Annu. Rev. Microbiol. 39*, 109–129.

Bazinet, C., & King, J. (1985b) *Virology 143*, 368–379.

Bazinet, C., & King, J. (1988) *J. Mol. Biol.* (in press).

Berget, P. B., & Poteete, A. R. (1980) *J. Virol. 34*, 234–243.

Black, L. W., & Showe, M. K. (1983) in *Bacteriophage T4* (Mathews, E. M., Kutter, G., Mosig, G., & Berget, P. B., Eds.) pp 219–245, American Society for Microbiology, Washington, DC.

Botstein, D., Waddell, C. H., & King, J. (1973) *J. Mol. Biol. 80*, 669–695.

Bradford, M. M. (1976) *Anal. Biochem. 72*, 248–254.

Camacho, A., Jimenez, F., De La Torre, J., Carrascosa, J. L., Mellado, R. P., Vasquez, C., Vinuela, E., & Salas, M. (1977) *Eur. J. Biochem. 73*, 39–55.

Carazo, J. M., Garcia, N., Santisteban, A., & Carrascosa, J. L. (1984) *J. Ultrastruct. Res. 89*, 79–88.

Carazo, J. M., Santisteban, A., & Carrascosa, J. L. (1985) *J. Mol. Biol. 183*, 79–88.

Carazo, J. M., Fujisawa, H., Nakasu, S., & Carrascosa, J. L. (1986a) *J. Ultrastruct. Mol. Struct. Res. 94*, 105–113.

Carazo, J. M., Donate, L. E., Herranz, L., Secilla, J. P., & Carrascossa, J. L. (1986b) *J. Mol. Biol. 192*, 853–867.

Carrascosa, J. L., Vinuela, E., Garcia, N., & Santisteban, A. (1982) *J. Mol. Biol. 154*, 311–324.

Carrascosa, J. L., Carazo, J. M., & Garcia, N. (1983) *Virology 124*, 133–143.

Carrascosa, J. L., Carazo, J. M., Ibanez, C., & Santisteban, A. (1985) *Virology 141*, 190–200.

Casjens, S., & King, J. (1974) *J. Supramol. Struct. 2*, 202–224.

Casjens, S., & Huang, W. M. (1982) *J. Mol. Biol. 157*, 287–298.

Crowther, R. A., & Amos, L. A. (1971) *J. Mol. Biol. 60*, 123–130.

Driedonks, R. A., Engel, A., ten-Heggeler, B., & van Driel, R. (1981) *J. Mol. Biol. 152*, 641–662.

Earnshaw, W., & King, J. (1978) *J. Mol. Biol. 126*, 721–747.

Earnshaw, W., & Casjens, S. (1980) *Cell (Cambridge, Mass.) 21*, 319–331.

Earnshaw, W., Casjens, S., & Harrison, S. C. (1976) *J. Mol. Biol. 104*, 387–410.

Edelhoch, H. (1960) *J. Biol. Chem. 235*, 1326–1334.

Edsall, J. T. (1953) in *The Proteins* (Neurath, H., & Baily, K., Eds.) pp 549–726, Academic, New York.

Fairbanks, G., Steck, T. L., & Wallach, D. F. H. (1971) *Biochemistry 10*, 2606–2617.

Feiss, M., & Becker, A. (1983) in *Lambda II* (Hendrix, R. W., Roberts, J. W., Stahl, F. W., & Weisberg, R. A., Eds.) pp 305–330, Cold Spring Harbor Laboratory, Cold Spring Harbor, NY.

Fuller, M. T., & King, J. (1981) *Virology 112*, 529–547.

Fuller, M. T., & King, J. (1982) *J. Mol. Biol. 156*, 633–665.

Georgopoulos, C., Tilly, K., & Casjens, S. (1983) in *Lambda II* (Hendrix, R. W., Roberts, J. W., Stahl, F. W., & Weisberg, R. A., Eds.) pp 279–304, Cold Spring Harbor Laboratory, Cold Spring Harbor, NY.

Hagen, E. W., Reilly, B. E., Tosi, M. E., & Anderson, D. L. (1977) *J. Virol. 19*, 501–517.

Hartwieg, E., Bazinet, C., & King, J. (1986) *Biophys. J. 49*, 24–26.

Hendrix, R. (1978) *Proc. Natl. Acad. Sci. U.S.A. 75*, 4779–4783.

Hess, E. L., & Deutsch, H. F. (1948) *J. Am. Chem. Soc. 70*, 84–88.

Hodgkin, D. C., Pickworth, J., Robertson, J. H., Trueblood, K. N., Prosen, R. J., & White, J. G. (1955) *Nature (London) 176*, 325–328.

Horne, R. W., & Pasquali Ronchetti, I. (1974) *J. Ultrastruct. Res. 47*, 361–383.

Hsiao, C. L., & Black, L. W. (1977) *Proc. Natl. Acad. Sci. U.S.A. 74*, 3652–3656.

Hsiao, C. L., & Black, L. W. (1978a) *Virology 91*, 15–25.

Hsiao, C. L., & Black, L. W. (1978b) *Virology 91*, 26–38.

King, J., & Casjens, S. (1974) *Nature (London) 251*, 112–119.

King, J., Lenk, E. V., & Botstein, D. (1973) *J. Mol. Biol. 80*, 697–731.

King, J., Botstein, D., Casjens, S., Earnshaw, W., Harrison, S., & Lenk, E. (1976) *Philos. Trans. R. Soc. London, B 276*, 37–49.

Kochan, J., & Murialdo, H. (1983) *Virology 131*, 100–115.

Kochan, J., Carrascosa, J. L., & Murialdo, H. (1984) *J. Mol. Biol. 174*, 433–447.

Laemmli, U. K. (1970) *Nature (London) 227*, 680–685.

Laemmli, U. K., & Eiserling, F. A. (1968) *Mol. Gen. Genet. 101*, 333–345.

Lenk, E., Casjens, S., Weeks, J., & King, J. (1975) *Virology 68*, 182–199.

Martin, R., & Ames, B. (1961) *J. Biol. Chem. 236*, 1372–1397.

Moody, M. F. (1965) *Virology 26*, 567–576.

Moody, M. F. (1973) *J. Mol. Biol. 80*, 613–635.

Muller-Salamin, L., Onorato, L., & Showe, M. K. (1977) *J. Virol. 24*, 121–134.

Murialdo, H., & Becker, A. (1977) *Proc. Natl. Acad. Sci. U.S.A. 74*, 907–910.

Murialdo, H., & Becker, A. (1978a) *Microbiol. Rev. 42*, 529–576.

Murialdo, H., & Becker, A. (1978b) *J. Mol. Biol. 125*, 57–74.

Poteete, A. R., & King, J. (1977) *Virology 76*, 725-739.
Poteete, A. R., Jarvik, V., & Botstein, D. (1979) *Virology 95*, 550-564.
Strauss, H., & King, J. (1984) *J. Mol. Biol. 172*, 523-543.
Susskind, M. M. (1980) *J. Mol. Biol. 138*, 685-713.
Susskind, M. M., & Botstein, D. (1978) *Microbiol. Rev. 42*, 385-413.
Susskind, M., Botstein, D., & Wright, A. (1974) *Virology 62*, 350-366.
Thomas, G. J., Li, Y., Fuller, M. T., & King, J. (1982) *Biochemistry 21*, 3860-3878.
Tsui, L., & Hendrix, R. W. (1980) *J. Mol. Biol. 142*, 419-438.
Yanagida, M., Suzuki, Y., & Toda, T. (1984) *Adv. Biophys. 17*, 97-146.
Youderian, P., & Susskind, M. M. (1980) *Virology 107*, 258-269.

Hydrophobic Photolabeling Identifies BHA2 as the Subunit Mediating the Interaction of Bromelain-Solubilized Influenza Virus Hemagglutinin with Liposomes at Low pH†

Cordula Harter,‡ Thomas Bächi,§ Giorgio Semenza,‡ and Josef Brunner*,‡

Laboratorium für Biochemie der Eidgenössischen Technischen Hochschule, ETH-Zentrum, CH-8092 Zürich, Switzerland, and Institut für Immunologie und Virologie der Universität Zürich, Gloriastrasse 30, CH-8028 Zürich, Switzerland

Received July 22, 1987; Revised Manuscript Received November 2, 1987

ABSTRACT: To investigate the molecular basis of the low-pH-mediated interaction of the bromelain-solubilized ectodomain of influenza virus hemagglutinin (BHA) with membranes, we have photolabeled BHA in the presence of liposomes with the two carbene-generating, membrane-directed reagents 3-(trifluoromethyl)-3-(*m*-[^{125}I]iodophenyl)diazirine ([^{125}I]TID) and a new analogue of a phospholipid, 1-palmitoyl-2-[11-[4-[3-(trifluoromethyl)diazirinyl]phenyl][2-^{3}H]undecanoyl]-*sn*-glycero-3-phosphocholine ([^{3}H]-PTPC/11). With the latter reagent, BHA was labeled in a strictly pH-dependent manner, i.e., at pH 5 only, whereas with [^{125}I]TID, labeling was seen also at pH 7. In all experiments, the label was selectively incorporated into the BHA2 polypeptide, demonstrating that the interaction of BHA with membranes is mediated through this subunit, possibly via its hydrophobic N-terminal segment. Similar experiments with a number of other water-soluble proteins (ovalbumin, carbonic anhydrase, α-lactalbumin, trypsin, and soybean trypsin inhibitor) indicate that the ability to interact with liposomes at low pH is not a property specific for BHA but is observed with other, perhaps most, proteins.

The fusion of membranes is an essential step in a broad range of biological processes such as intracellular transport, endocytosis, exocytosis, fertilization, and the entry of genome of enveloped animal viruses into the host cell. There have been extensive investigations concerning the mechanism and specificity of membrane fusion. Yet the molecular mechanisms are not, or only poorly, understood. In many cases, Ca^{2+} ions are required while in some others, the fusion process is triggered solely by proteins (Papahadjopoulos et al., 1977, 1979; White et al., 1983). Recently, Lucy proposed that fusion in biological systems is mediated by hydrophobic protein segments that result from endogenous proteolyses (Lucy, 1984). In the case of enveloped animal viruses, specific fusion proteins have been identified (White et al., 1983). On the other hand, there is evidence that membrane fusion can also be triggered effectively by several water-soluble proteins such as cytochrome *c* (Gad et al., 1982), clathrin (Hong et al., 1985), lysozyme (Arvinte et al., 1986), and α-lactalbumin (Kim & Kim, 1986), suggesting that fusion is a more general phenomenon than anticipated earlier.

Entry of influenza viruses into cells is mediated by a low-pH-induced membrane fusion event in endosomal vesicles (Skehel et al., 1982). The factor responsible for fusion is hemagglutinin (HA),[1] a viral spike protein whose structure is exceptionally well characterized. HA is a trimeric transmembrane protein in which each subunit consists of two disulfide-linked glycopeptides HA1 and HA2 with molecular weights of 58 000 and 26 000, respectively (Klenk et al., 1975; Wiley et al., 1977; Lazarowitz & Choppin, 1975). Exhaustive

† This work was supported by a research grant from the Swiss National Science Foundation, Bern (3.228-0.85 to J.B.).
* Address correspondence to this author.
‡ Laboratorium für Biochemie der Eidgenössischen Technischen Hochschule.
§ Institut für Immunologie und Virologie der Universität Zürich.

[1] Abbreviations: HA, influenza virus hemagglutinin; BHA, BHA1, and BHA2, bromelain-solubilized ectodomain of HA (BHA) and the two subunits derived therefrom; [^{125}I]TID, 3-(trifluoromethyl)-3-([^{125}I]-iodophenyl)diazirine; [^{3}H]PTPC/8, 1-palmitoyl-2-[11-[4-[(trifluoromethyl)diazirinyl]phenyl][10-^{3}H]-9-oxaundecanoyl]-*sn*-glycero-3-phosphocholine; [^{3}H]PTPC/11, 1-palmitoyl-2-[11-[4-[3-(trifluoromethyl)diazirinyl]phenyl][2-^{3}H]undecanoyl]-*sn*-glycero-3-phosphocholine; DPPC, dipalmitoyllecithin; TLC, thin-layer chromatography; DMF, dimethylformamide; THF, tetrahydrofuran; EDTA, ethylenediaminetetraacetic acid; MES, 2-(*N*-morpholino)ethanesulfonic acid; SDS, sodium dodecyl sulfate; Tris, tris(hydroxymethyl)aminomethane; PBS, 150 mM NaCl and 5 mM sodium phosphate; SBTI, soybean trypsin inhibitor; PC, 1,2-diacyl-*sn*-glycero-3-phosphocholine; PS, 1,2-diacyl-*sn*-glycero-3-phosphoserine; PE, 1,2-diacyl-*sn*-glycero-3-phosphoethanolamine.

0006-2960/88/0427-1856$01.50/0